

# ACCOUNTS of CHEMICAL RESEARCH®

JULY 2003

Registered in U.S. Patent and Trademark Office; Copyright 2003 by the American Chemical Society

## Real-Time Observation of Surface Reactivity and Mobility with Scanning Tunneling Microscopy

XING-CAI GUO AND ROBERT J. MADIX\*  
Departments of Chemical Engineering and Chemistry,  
Stanford University, Stanford, California 94305-5025

Received September 3, 2002 (Revised Manuscript Received January 20, 2003)

### ABSTRACT

Scanning tunneling microscopy allows the direct observation of reactions on surfaces on the atomic scale that otherwise must be inferred from the statistical behavior of hundred of trillions of molecules or atoms. Since the study of the details of reactions on this length scale began, our conception of surface reactivity has changed profoundly. In this Account we focus attention on our real-time observations of reactions for a number of systems, including the island growth of surface oxide on Cu(110), the anisotropic and site-specific reactivity of this oxide with carbon monoxide and ammonia, the collective motion of laterally interacting O(a) and SO<sub>3</sub>(a), and the incorporation of metal atoms into the structures of molecular intermediates formed in the reaction of ammonia with O(a) on Ag(110). These nanoscale, time-resolved movies capture the events as they occur, providing a dynamic picture of the distribution of reactants and products on the surface, thus providing a better understanding of the roles of reactant distribution and site specificity in surface reactivity.

### 1. Introduction

The time-dependent behavior of chemical reactions has captivated many scientists throughout history.<sup>1</sup> In the mid-19th century, Wilhelmy first measured quantitatively

X.-C. Guo received his Ph.D. in chemistry in 1990 from University of Pittsburgh under Professor J. T. Yates, Jr. He was then awarded a three-year Openheimer and a one-year Humboldt fellowship. He took the longer fellowship at University of Cambridge under Professor D. A. King. His collaboration with Professor R. J. Madix began in late 1993, which continued after two years as an associate professor and professor at the University of Petroleum in China. Presently he is a staff scientist in Professor Madix's laboratory at Stanford University. His research interests lie in the broad areas of surface science, materials science, semiconductor and computer science, and nanoscience and technology.

the rate of hydrolysis of sucrose. Then Harcourt and Esson carried out experiments with reactions between H<sub>2</sub>O<sub>2</sub> and HI and between KMnO<sub>4</sub> and (COOH)<sub>2</sub> and analyzed the concentration (*c*) of reactants versus time (*t*). In his book "Études de dynamique chimique" published in 1884, van't Hoff generalized these analyses, using many results obtained in his own laboratory for reactions, such as the decomposition of arsine in the gas phase and the hydrolysis of ethyl acetate by caustic soda. He recognized the significance of the reaction order, *n*, as in

$$-dc/dt = kc^n \quad (1)$$

where *k* is the rate constant independent of concentration. By argument and curve-fitting, van't Hoff arrived at an empirical equation

$$k = Ae^{-E/RT} \quad (2)$$

where *A* and *E* are constants independent of the temperature (*T*). Five years later Arrhenius gave *E* an interpretation as the energy barrier to reaction, and the equation has thus come to be called the "Arrhenius equation".<sup>1</sup> As a result of this interpretation, several other empirical equations were discarded, although they all fit the experimental data equally well. In the 20th century, theories were proposed to interpret and predict the preexponential factor (*A*) in the Arrhenius equation, notably collision theory and transition state theory. The equations for reaction rates and rate constant have been used success-

\* Corresponding author. E-mail rjm@chemeng.stanford.edu.

R. J. Madix received his Ph.D. in chemical engineering in 1964 from University of California at Berkeley. After a year as an NSF postdoctoral fellow at Max Planck Institute for Physical Chemistry in Germany, he became an assistant professor, associate professor, and professor in the Department of Chemical Engineering at Stanford University. He has also been a professor of chemistry since 1981 and the Charles Lee Powell Professor in the School of Engineering since 1995. Among his honors are the Humboldt Senior Scientist Award, the ACS Langmuir Distinguished Lectureship Award, the Emmett Award in Fundamental Catalysis, the Debye Lectureship, the AIChE Alpha Chi Sigma Award, the Eyring Lectureship in Chemistry, and the ACS Adamson Award in Surface Chemistry. His current research activities include microscopically imaging molecular reactions on metal surfaces, model studies of reactions on metal oxide surface, and dynamic studies of adsorption on metal surfaces.

fully to describe numerous types of reactions in homogeneous phases.

However, such simple analytical descriptions do not necessarily apply to reactions in all phases. Arbitrary use of the equations often generates concentration and/or temperature-dependent values of  $E$  and  $A$ , which actually invalidate their use. Various modifications of the equations have thus been made, which inevitably introduce more fitting parameters that are open to further interpretation. Obviously, if two liquids are immiscible or, similarly, if two adsorbates on a surface segregate into separate phases, reaction may occur only at the phase boundaries. A single overall concentration or coverage does not adequately describe the concentration dependence of the rate equation for such a system. Thus, reactions in condensed phases can be accompanied by a complex distribution of reactants that render assumptions carried over from the usual description of homogeneous reactions inappropriate.

The kinetics of reactions on an ordinary single-crystal surface ( $\sim 0.25 \text{ cm}^2$ ) is the result of the interplay of about a hundred trillion ( $10^{14}$ ) molecules or atoms. Today, using a scanning tunneling microscope (STM), one can directly see the distribution of individual molecules or atoms on the nanometer scale. Since the onset of our quest to image surface reactions on this length scale, our concept of the nature of surface reactivity has undergone a profound change. The purpose of this article is to share some of these shifts in paradigms with the larger chemistry community.

Resolution on the nanometer scale has been the trademark of STM since its invention.<sup>2</sup> Recent advances in STM instrumentation have produced recording rates up to 20 frames per second.<sup>3</sup> A series of STM images of the same surface area can be recorded to produce a movie of events occurring on the atomic scale. In this Account we focus on matters related to surface reactions, taking single frames from five STM movies produced in our laboratory at various recording rates. These include (1) the island growth of a surface oxide resulting from  $\text{O}_2$  adsorption on Cu(110), (2) the anisotropic reactivity of these islands with CO, (3) the site-specific reactivity of  $\text{NH}_3$  in reactions with adsorbed oxygen on Cu(110), (4) the collective motion of O(a) and  $\text{SO}_3$ (a) on Cu(110), and (5) the incorporation of "extra" metal atoms into the unit cell of a reaction intermediate in the reaction of  $\text{NH}_3$  with adsorbed oxygen on Ag(110). The STM movies may be directly viewed at our website.<sup>4</sup> These nanoscale movies captured the events as they occur, helping us to visualize the dynamic reactant distributions.

## 2. The Crystallization of a Two-Dimensional Oxide: Oxygen Adsorption on Cu(110)<sup>5</sup>

It has been known for some time that the dissociative adsorption of oxygen on Cu(110) at room temperature produces a unit cell structure with lattice vectors different from those of the clean surface, forming a  $p(2 \times 1)$  phase.<sup>6</sup> (The  $(2 \times 1)$  notation denotes that the two-dimensional unit

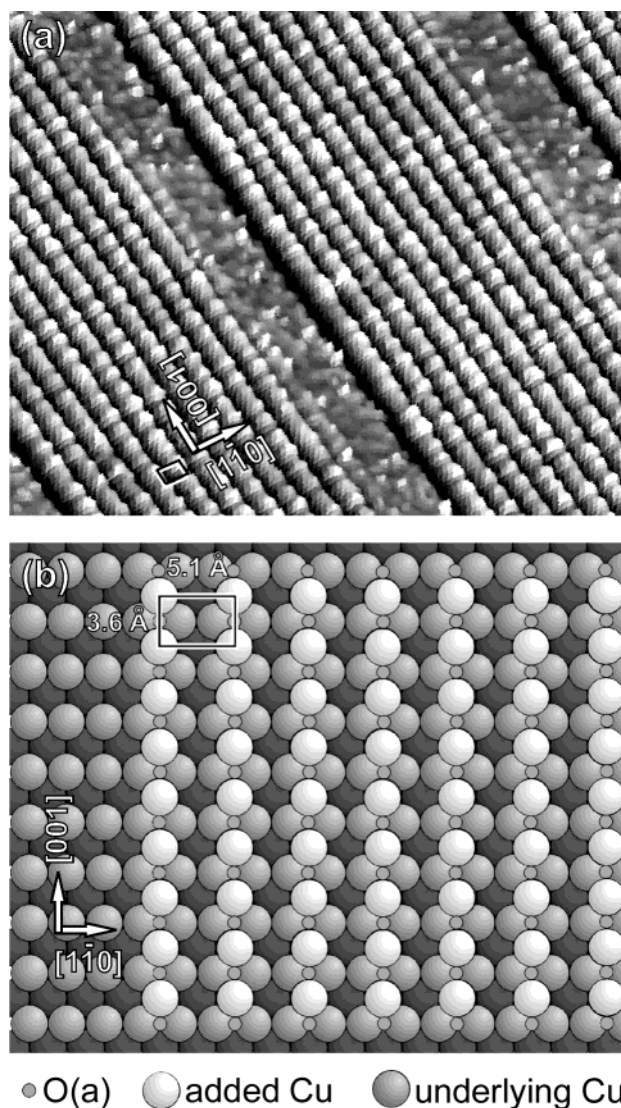
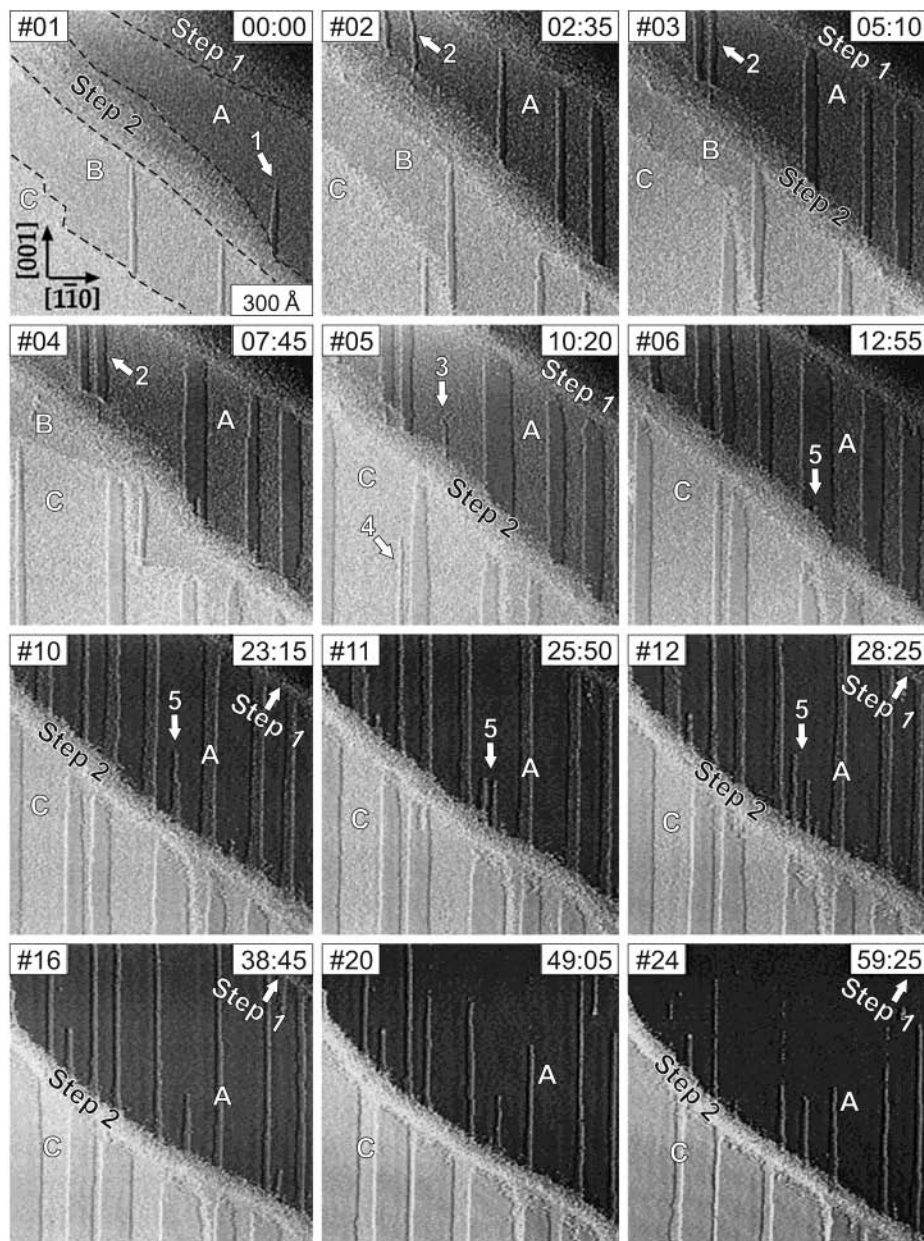


FIGURE 1. STM image (top) of the  $p(2 \times 1)$ -O structure on Cu(110) and a ball model (below) showing the added  $-\text{Cu}-\text{O}-$  rows.

cell that the adsorbed oxygen adopts has lattice vectors that are 2 and 1 times the unit cell vectors of the clean surface structure, having the same directions.) Overlayer structures having periodicities differing from that of the underlying host metal are common, but the process leading to this particular structure on Cu(110), as disclosed by STM, was quite unexpected.<sup>7-9</sup> After the dissociation of molecular oxygen on the Cu(110) surface, oxygen atoms combine with mobile Cu atoms that are either released from step edges or from the terraces themselves to form added  $-\text{Cu}-\text{O}-$  rows along the [001] direction. The  $-\text{Cu}-\text{O}-$  rows coalesce to form islands of  $p(2 \times 1)$ -O structure with gaps of clean surface between the islands.<sup>7-10</sup> One such STM image is shown in Figure 1 with a ball model below. Only Cu atoms in the rows are imaged; oxygen atoms are invisible under the particular imaging conditions.<sup>8,9,11</sup> The coverage of oxygen atoms in the  $p(2 \times 1)$ -O structure is 0.5 ML (monolayer, 1 ML = 1 O/Cu).

To gain a more detailed picture of the island growth process, we have followed the buildup of oxygen on Cu(110) from 0.0 to 0.5 ML.<sup>5</sup> Figure 2 displays 12 selected



**FIGURE 2.** Selected frames of STM images recorded sequentially at a scan rate of 155 s per frame in an ambient oxygen pressure of  $2.5 \times 10^{-9}$  Torr at 470 K on Cu(110).

STM images recorded sequentially 155 s apart in an ambient oxygen pressure of  $2.5 \times 10^{-9}$  Torr at a surface temperature of 470 K. In the first image obtained after oxygen exposure was commenced, three terraces at different heights can be distinguished. A bundle of several steps running diagonally from the upper left to the lower right separate the lowest- and mid-lying terraces (A and B), while a monatomic step separates the mid- and highest-lying terraces (B and C).

Overall, three stages of growth can be distinguished: nucleation, growth, and coalescence. As seen in frame 1, the initial growth proceeds from the bottom of the step and proceeds over the terrace (arrow 1). Soon after the first islands form, additional islands appear on the terraces (frame 2). Two initially separated islands attract with each other and become paired at the upper left corner of

terrace A in frames 2–4 (arrow 2). The nucleation of new islands takes place only below 0.2 ML (frame 5, arrow 3). On terrace C a thin band (arrow 4) appears adjacent to an oxide island.

The islands grow in a correlated fashion, not completely randomly. The growth of terrace C is seen in the first five frames. The additional Cu atoms appear to be supplied from the broad bundle of steps (step 2) separating terraces A and B, which retracts continuously toward the lower left corner of the image view, eventually eliminating the middle terrace (B). The island growth along the [001] direction occurs over the whole terrace width on the time scale of the imaging of one frame. It is clear from the splitting at the ends of the islands adjacent to the step (arrow 5 in frames 6–12) that material transport to and

from the end of the islands at the steps is intimately involved in their growth.

When the spacing between neighboring islands reaches about 20 Å, the islands start to coalesce simultaneously on terrace A (frame 20). As shown in frames 20 and 24, on terrace A the remaining gaps appear to fill from step 1 toward step 2, suggesting that  $-\text{Cu}-\text{O}-$  moieties are produced at step 2 and diffuse to the end of the gaps.

### 3. Anisotropic Reactivity: Oxidation of Carbon Monoxide on Cu(110)<sup>12</sup>

The catalytic oxidation of CO to CO<sub>2</sub> on the  $p(2\times 1)$ -O-covered Cu(110) proceeds via the reaction between coadsorbed CO and oxygen<sup>13–16</sup>



CO<sub>2</sub> is so weakly bound to the surface that even at room temperature it desorbs from the surface upon formation. There are two types of oxygen accessible at an island perimeter: oxygen atoms at the end of a  $-\text{Cu}-\text{O}-$  row or island and oxygen atoms within a row on the side of an island. An equilibrium population of interstitial oxygen adatoms must also exist. Previously it was estimated that the rate of removal of oxygen from the end of a row along the [001] direction was only twice as likely as that along the  $[\bar{1}10]$  direction—a rather small difference in reactivity.<sup>13,14</sup> STM allows us to probe this difference directly.

Under steady state conditions the distribution of reactants on the surface is quite dynamic. On a local scale, significant fluctuations in island size and shape are observed, as oxygen is continuously removed and replenished at the boundaries of the oxide islands. The length and width of islands change, and the addition and removal of oxide strands at the perimeter of the islands create both point and line defects. Shown in Figure 3 are STM images selected from a time-lapse series taken 155 s apart for the oxidation of CO under near steady-state conditions with the surface at 400 K. Both CO and O<sub>2</sub> are present in the gas phase with a total pressure of about  $2 \times 10^{-4}$  Torr.

The imaged area is neatly marked by a kink in a step separating two terraces (frame 1, upper left). The four  $p(2\times 1)$ -O islands (dark gray) identified by arrows 1–4 in frame 1 on the upper terrace are the focus of discussion here. Similar behavior is seen on the other terraces. The length of island 1 (arrow 1), initially two  $-\text{Cu}-\text{O}-$  rows in width, first increases (frames 1–2) and then decreases (frames 3–10), eventually passing from view (frame 24). An island nucleates near the step edge (frames 25–32, arrow 5). It grows in both length and thickness; the forked structure at the end of this island (frame 32, arrow 5) is a clear indication of the deposition and erosion of material from its tip. Arrow 2 marks the end of the left-most row in a  $p(2\times 1)$ -O island consisting of three  $-\text{Cu}-\text{O}-$  rows (frame 1). This row is reacted away initially (frame 2) but is then regenerated (frame 3). The fluctuation of the

boundary of this island continues (frames 8–32, arrow 2). These fluctuations are particularly evident in frames 27–32. Similar behavior is exhibited for island 3 (arrow 3). The jagged edges of this island (arrow 3), representing the end of  $-\text{Cu}-\text{O}-$  rows, fluctuate in width and position through all frames. Oxide strands appear and disappear from the island boundary with time. This island doubles in width over the course of the observation. Generally similar behavior is observed for island 4.

The formation of the jagged edges at the island boundary and their continual fluctuation suggest that preferential reaction and aggregation of oxygen occurs at the defect sites along the island perimeter. The fluctuating lengths of the  $-\text{Cu}-\text{O}-$  rows at the island perimeter indicate that CO reacts with oxygen primarily along the row in the [001] direction. The reaction anisotropy can be attributed to the lesser stability of an oxygen atom at a row end or at a kink site at the island edge than that within the row. The evolution of island shape during reaction has been compared to Monte Carlo simulations.<sup>12</sup> It suggests that the reaction probability at the end of an island is 500–1000 times greater than that at the side.

### 4. Site-Specific Reactivity of Atomic Oxygen Species: Ammonia on Cu(110)- $p(2\times 1)$ -O<sup>17</sup>

The reactions between ammonia and oxygen on Cu(110) have been investigated previously using high-resolution electron energy loss spectroscopy (HREELS)<sup>18,19</sup> and X-ray photoelectron spectroscopy (XPS).<sup>19</sup> It was initially reported that there was no reactivity between preadsorbed oxygen in the fully covered  $p(2\times 1)$ -O structure. It was then found that exposure of Cu(110) at 300 K to a gas mixture of ammonia and oxygen results in the highly selective oxydehydrogenation reaction to form imide, NH(a). The differences in reactivity were hypothesized to reside in two distinctly different oxygen species: an “inherently unreactive” oxygen species analogous to preadsorbed  $p(2\times 1)$ -O structure, and an oxygen transient similar to that produced in the co-exposure experiment.<sup>20</sup> Though these transient species are clearly quite reactive,<sup>21</sup> our STM observations of this system provide direct evidence that the oxygen in the preadsorbed  $p(2\times 1)$ -O structure is also reactive. Extensive reaction can be inhibited by the accumulation of NH(a).

In our experiments the Cu(110) surface was initially partly covered by  $p(2\times 1)$ -O islands with an overall oxygen coverage of  $\sim 0.3$  ML. After exposure to ammonia at 300 K, the surface was heated to 410 K and cooled to 300 K at an ambient ammonia pressure of  $\sim 2 \times 10^{-9}$  Torr. Under these conditions the surface NH(a) is expected to be stable, if reaction proceeds.<sup>18,19</sup> The surface was then imaged with STM at 300 K (Figure 4a). The thinner rows along the [001] direction are  $-\text{Cu}-\text{O}-$  rows, and the thicker rows along the  $[\bar{1}10]$  direction are attributed to NH(a) species. The presence of NH(a) structures and the appearance of  $p(2\times 1)$ -O islands with irregular edges indicate that the preadsorbed oxygen islands are reactive with ammonia. The reactions are initiated near the step

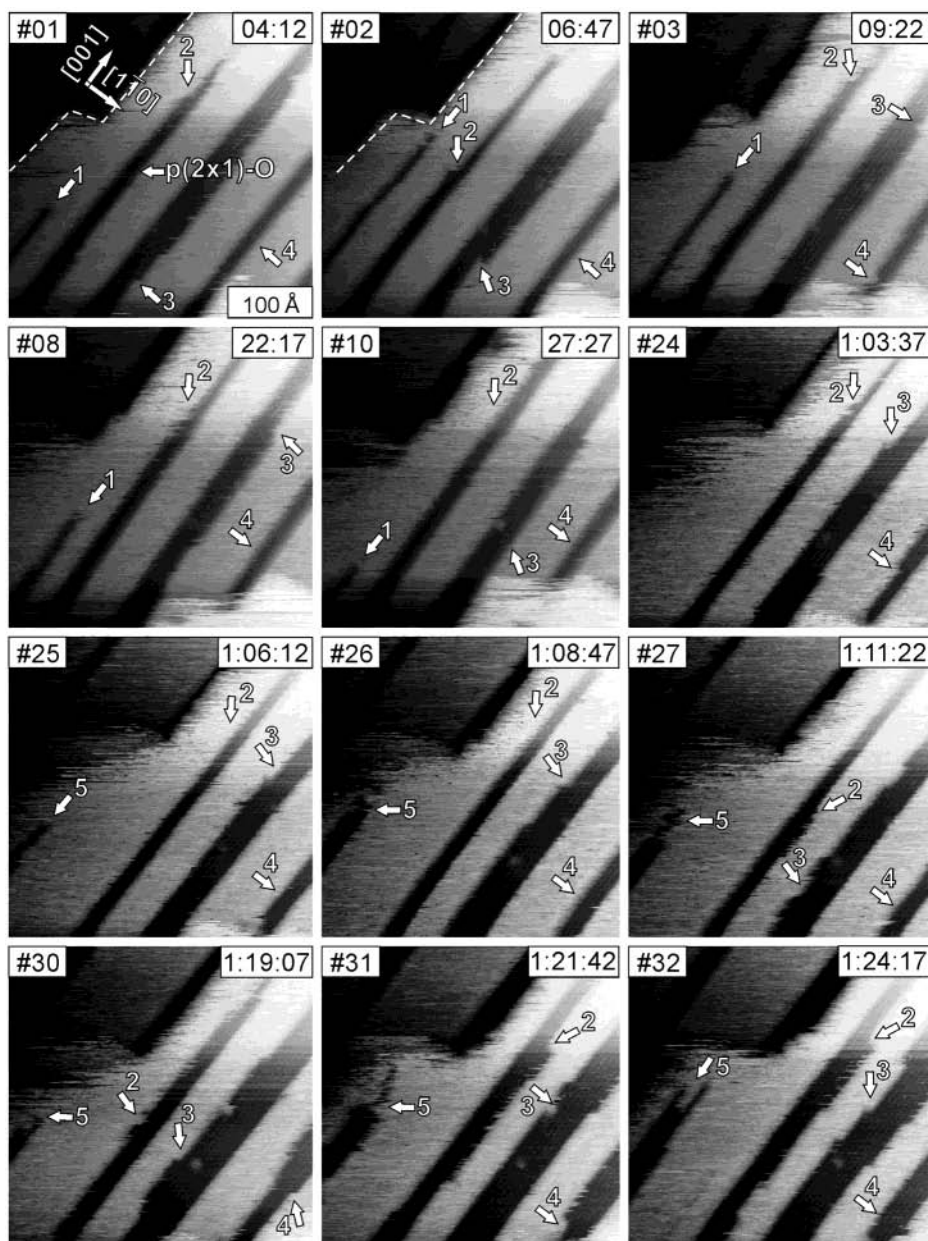


**FIGURE 3.** Selected frames of STM images recorded sequentially at a scan rate of 155 s per frame during the oxidation of CO on Cu(110) under near steady-state conditions with the surface at 400 K.

edges. Some of the NH(a) rows intercept and terminate  $-\text{Cu}-\text{O}-$  rows, suggesting that reaction along the oxide row is inhibited by site-blocking. Such site blocking can significantly limit the extent of reaction of ammonia with the preadsorbed oxygen. Herein appears to rest the origin of the significant difference between the reactivity of preadsorbed oxygen and coadsorbed oxygen with ammonia.<sup>20</sup> This inhibiting effect is not seen in CO oxidation on this surface because the product of the reaction does not remain adsorbed. These inhibition effects and the effects of steps on the reactions have been discussed in detail elsewhere.<sup>22,23</sup>

The reaction of  $p(2\times 1)\text{-O}$  with ammonia proceeds anisotropically, reaction along the oxide strands being faster than reaction into the sides of the islands. However, reaction can be initiated at the island boundary. The boxed region with dashed lines in Figure 4a was moni-

tored in situ with STM at a scan rate of 205 s per frame under an ambient pressure of  $\text{NH}_3$  of  $2 \times 10^{-9}$  Torr. Selected frames are displayed in Figure 4. Frame 1 was recorded 1 h 8 min 20 s after the dashed frame shown in Figure 4. The two  $-\text{Cu}-\text{O}-$  rows marked by arrows 1 and 2 in Figure 4 have been shortened such that they lie within the dashed frame. Their shortening continues (Figure 4, frames 2–5) at an averaged rate of 4 atoms/min. These two  $-\text{Cu}-\text{O}-$  rows are reacted away along the rows from the ends such as a burning straw. A similar anisotropy has been reported for oxidation reactions of CO on Rh(110)<sup>24</sup> and Cu(110) (see above), methanol on Cu(110),<sup>25</sup> and ammonia on Ni(110).<sup>26</sup> In general the low-coordinated oxygen is removed preferentially from the island. Whether this is due to an inherently higher local reactivity or a lower stability is not clearly understood.<sup>12</sup>

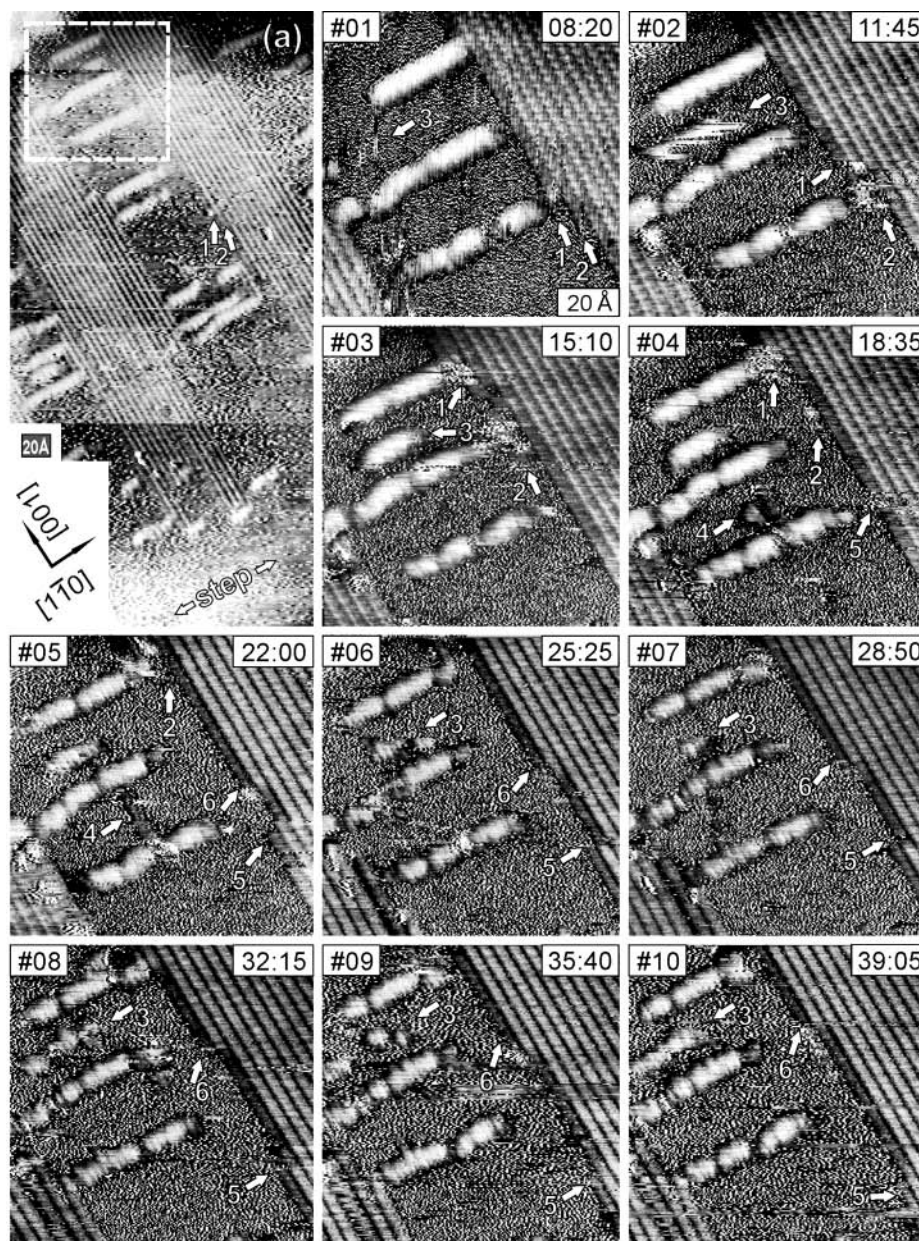


**FIGURE 4.** The boxed region with dashed lines in panel a was monitored with STM at a scan rate of 205 s per frame under an ambient pressure of  $\text{NH}_3$  of  $2 \times 10^{-9}$  Torr at 300 K on oxygen precovered Cu(110). Frames obtained at selected times are displayed.

A short NH(a) segment moves back and forth along the  $[110]$  axis like a worm (arrow 3), whereas other NH(a) strands appear to be immobile. The short NH(a) segment (arrow 3) breaks apart into two segments (frames 8 and 9), which reunite (frame 10). Although the growth of NH(a) segments was not observed within the small imaging area, the growth was seen in other regions during reactions.<sup>17</sup> A short  $-\text{Cu}-\text{O}-$  segment appears between two long NH(a) segment (frame 5, arrow 4); it may arise from mobile Cu-O units on the surface. Reaction appears to be initiated at the side of a  $-\text{Cu}-\text{O}-$  row (frame 4, arrow 5). The opening created in the row widens (frames 5–10, arrows 5 and 6) at an averaged rate of 1 atom/min. The reactivity of  $p(2 \times 1)\text{-O}$  islands with ammonia is clearly visible on an atomic scale.

## 5. Collective Motion of Surface Adsorbates: Oxygen and Sulfite on Cu(110)

In the interstitial space between  $p(2 \times 1)\text{-O}$  islands a  $-\text{Cu}-\text{O}-$  row often appears as an irregular zigzag shape because it has moved between two successive line-scans. Although the mobility of a  $-\text{Cu}-\text{O}-$  row is obvious, it is not clear how a row moves. In 1990, Ertl's group<sup>27</sup> suggested fragmented motion. Later in the same year, Besenbacher's group<sup>9</sup> favored the collective motion of an entire row, which was accepted the next year by Ertl's group.<sup>28</sup> However, two year later Besenbacher dismissed the notion as "unlikely" and suggested that row motion proceeds as a series of correlated jumps of individual atoms.<sup>29</sup> Recently we acquired an STM movie of the motion of oxygen and

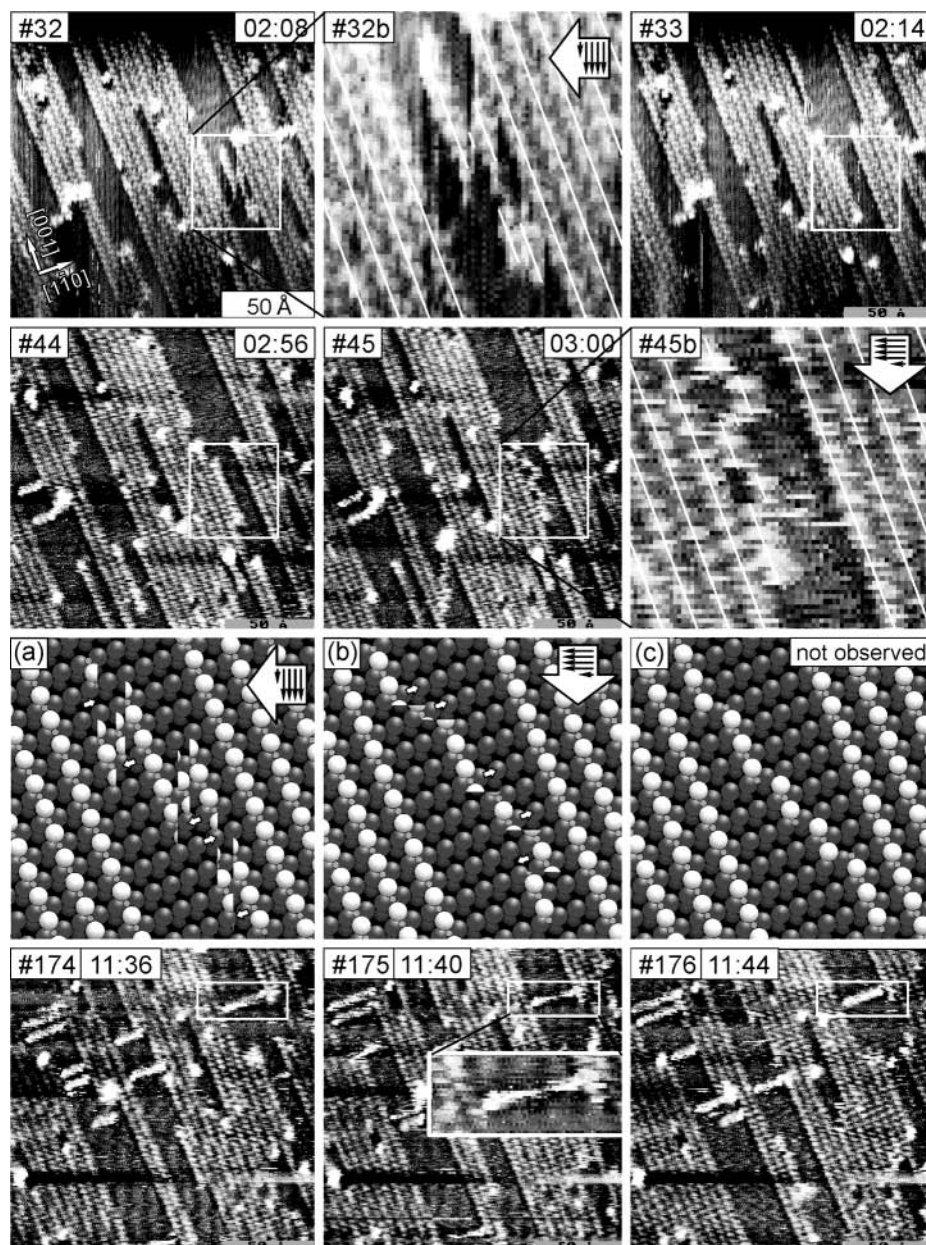


**FIGURE 5.** Selected frames of an STM movie recorded at 300 K while the Cu(110) surface (covered with 0.24 ML of oxygen) was exposed to  $\text{SO}_2$  at a pressure of  $1 \times 10^{-9}$  Torr. The scan rate was about 4 s per frame with a total of 257 frames. (a and b) Schematic illustrations of images resulting from vertical and horizontal scanning, respectively, while a  $-\text{Cu}-\text{O}-$  row is moving. (c) Fragmented motion or individual motion irrespective of scanning directions.

sulfite rows on Cu(110).<sup>11</sup> The  $-\text{Cu}-\text{O}-$  and  $\text{SO}_3$  rows seen in the movie appeared to move by a reptilian mechanism. However, detailed analysis of the images reveals evidence for collective motion of an entire row.

Figure 5 displays snapshots selected from a movie recorded while the Cu(110)-O surface was exposed to  $\text{SO}_2$  at a pressure of  $1 \times 10^{-9}$  Torr. A frame-by-frame analysis reveals interesting details of the collective row motion for both the  $-\text{Cu}-\text{O}-$  rows (along the [001] direction) and the  $\text{SO}_3$  rows (along the [110] direction). A boxed area in frame 32 is expanded in frame 32b, which shows a zigzag appearance of a short  $-\text{Cu}-\text{O}-$  row captured by the STM tip scanned top-to-bottom leftward, as indicated by the arrows in the upper right-hand corner. As a guide to the

eye, white lines are drawn on top of the rows with spacing of either one or two lattice units in the [110] direction. The row appears to shift up and down along the scan direction. The zigzag appearance disappears once the  $-\text{Cu}-\text{O}-$  row attaches to a  $p(2 \times 1)-\text{O}$  island (frame 33). The same row remains immobile while the STM scan direction changes from vertical to horizontal in frame 44. It appears zigzagged again in frame 45 when the area is scanned vertically, as shown more clearly in the expanded view in frame 45b. Again the zigzag shifts are along the scan direction, as the STM tip scans downward right to left.

Panels a and b of Figure 5 show schematic illustrations of images resulting from vertical and horizontal scanning,

respectively, while an entire  $-\text{Cu}-\text{O}-$  row is moving back-and-forth along the  $[\bar{1}10]$  direction (small white arrows). The motion gives rise to the zigzag appearance along the scanning direction as observed. The combination of both horizontally and vertically scanned STM images provides strong evidence for the collective motion of an entire  $-\text{Cu}-\text{O}-$  row. In contrast, fragmented motion or individual motion would appear zigzag along the  $[\bar{1}10]$  direction irrespective of scanning directions, as illustrated in Figure 5c. No such STM image was observed in any of over 250 frames. Similarly, frames 174–176 illustrate the collective motion of a  $\text{SO}_3$  row. Many other examples of this type are seen in the STM movie.

Theoretically, collective motion of interacting particles occurs in the presence of interactions, no matter how weak this interaction may be.<sup>30</sup> Collective motion occurs in nature on a wide range of time and length scale from bacteria to birds. In addition, the collective motion of the  $-\text{Cu}-\text{O}-$  rows on Cu(110) is not surprising if one thinks the  $-\text{Cu}-\text{O}-$  row as one entity or a pseudo-molecule.<sup>31</sup> Similar motion of the  $-\text{Ag}-\text{O}-$  rows has also been observed on Ag(110) surface.<sup>32</sup>

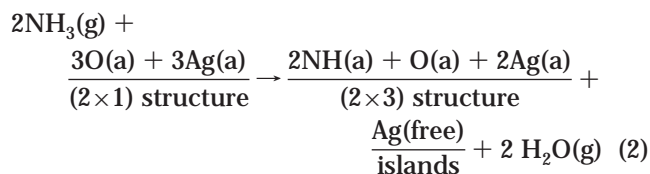
## 6. Molecular Intermediates Incorporate Metal Atoms: Ammonia on Ag(110)- $p(2 \times 1)$ -O<sup>33</sup>

On the Ag(110) surface, dioxygen reacts with the surface to form added  $-\text{Ag}-\text{O}-$  rows extending along the  $[001]$  direction,<sup>32</sup> much like those observed on Cu(110) (cf. Figure 1, bottom). Silver atoms are also incorporated into this overlayer structure. The saturated monolayer forms the  $p(2 \times 1)$ -O structure much like that of the Cu(110)- $p(2 \times 1)$ -O surface. As we found previously by temperature programmed reaction spectroscopy (TPRS) and high-resolution electron energy loss spectroscopy (HREELS),<sup>34</sup> reaction of ammonia with Ag(110)- $p(2 \times 1)$ -O at 300 K produces adsorbed OH(a) and NH(a), which, in turn, produce  $\text{H}_2\text{O}(\text{g})$ ,  $\text{NO}(\text{g})$ , and  $\text{N}_2(\text{g})$  when the surface is heated to higher temperatures. STM reveals a most unexpected sequence of events accompanying these reactions.

During the exposure of the Ag(110)- $p(2 \times 1)$ -O surface at 300 K to ammonia, a massive restructuring of the surface occurs, in which the added silver atoms in the oxide are released to form nanoscale islands, the entire surface being covered by NH(a). An STM movie was made of this process at a scan rate of 16 s/frame. Selected frames are displayed in Figure 6. As indicated in frame 1, the gray regions encircled by dashed lines are  $p(2 \times 1)$ -O regions, and the light gray stripes are due to NH(a) strings produced from reaction with background  $\text{NH}_3$  near the boundaries of the  $p(2 \times 1)$ -O regions. The stars mark the positions where silver islands (enclosed by dashed lines) nucleate, as the reaction proceeds; the islands grow, drawing silver atoms from the surrounding  $p(2 \times 1)$ -O regions. Generally speaking, these regions are initially defined by bordering NH(a). In all cases the presence of NH(a) was confirmed by higher resolution images (see below).<sup>33</sup>

Ammonia was introduced to the gas phase at  $4 \times 10^{-9}$  Torr. "Mottled" patches indicative of NH(a) grow initially at the boundaries of  $p(2 \times 1)$ -O islands (frame 23). Simultaneously, silver islands of monatomic height (dashed circles, labeled 1 and 2), covered by NH(a), nucleate at the top of the fame at the edges of NH(a) patches. These islands are clearly revealed by the shadows that extend from right to left. As the reaction proceeds (frame 27), island 1 expands into the area initially covered by  $p(2 \times 1)$ -O, while island 2 grows "downward" in the  $[001]$  direction into another area of  $p(2 \times 1)$ -O. Another nucleus (dash circle, labeled 3 in frame 27) appears, but its growth is hindered by surrounding NH(a) patches initially present, which neither supply silver atoms, nor permit silver atoms to migrate across them. The growth of islands 1 and 2 proceeds into the neighboring regions of  $p(2 \times 1)$ -O (frames 30 to 40). The emerging boundary of the NH(a) patches on the terrace appears to lead the front edge of the island growth by a few hundred angstroms (e.g., dashed line, frame 40), though the emerging reaction front is not perfectly aligned in the  $[001]$  direction. Eventually, growth of both islands 1 (frame 44) and 2 (frame 40) is arrested by the surrounding NH(a). As the growth of these islands is halted, new nuclei 4 (frame 40) and 5 (frame 44) appear, and the island growth process continues (frames 45–47). A zoomed-out view in frame 68 shows silver islands of various sizes ranging from a few nanometers to tens of nanometers. The silver islands are fairly randomly distributed over the entire surface. This result demonstrates that topographic restructuring occurs everywhere in a uniform manner. A zoomed-in view in Figure 6a on the right shows that NH(a) strands cover everywhere on terraces, including the top of silver islands.

The formation of the islands clearly indicates that there is a net loss of silver atoms in the reaction of ammonia with the added  $p(2 \times 1)$ -O structure to form NH(a). These silver atoms either nucleate into islands or migrate to step edges. The highest island coverage reached in this reaction was 16.4%. Additional high-resolution STM images show that the NH(a) induces a  $(2 \times 3)$  periodicity (Figure 6b).<sup>33</sup> The details of these studies suggest that a structure forms in which a  $(2 \times 3)$  Ag–O unit cell initially containing six top-layer Ag atoms incorporates two added Ag atoms, one O atom, and two NH(a) species (Figure 6c). This structure accounts for a net loss of Ag atoms from a  $(2 \times 3)$  cell of the oxygen overlayer, which contains three added Ag atoms. Thus, the reaction releases 1/6 of the added Ag atoms in the  $p(2 \times 1)$ -O structure to create NH(a)-covered Ag islands, which correspondingly cover 16.7% of the surface area, in agreement with the STM observations. Therefore, the following reaction is suggested to occur at 300 K:





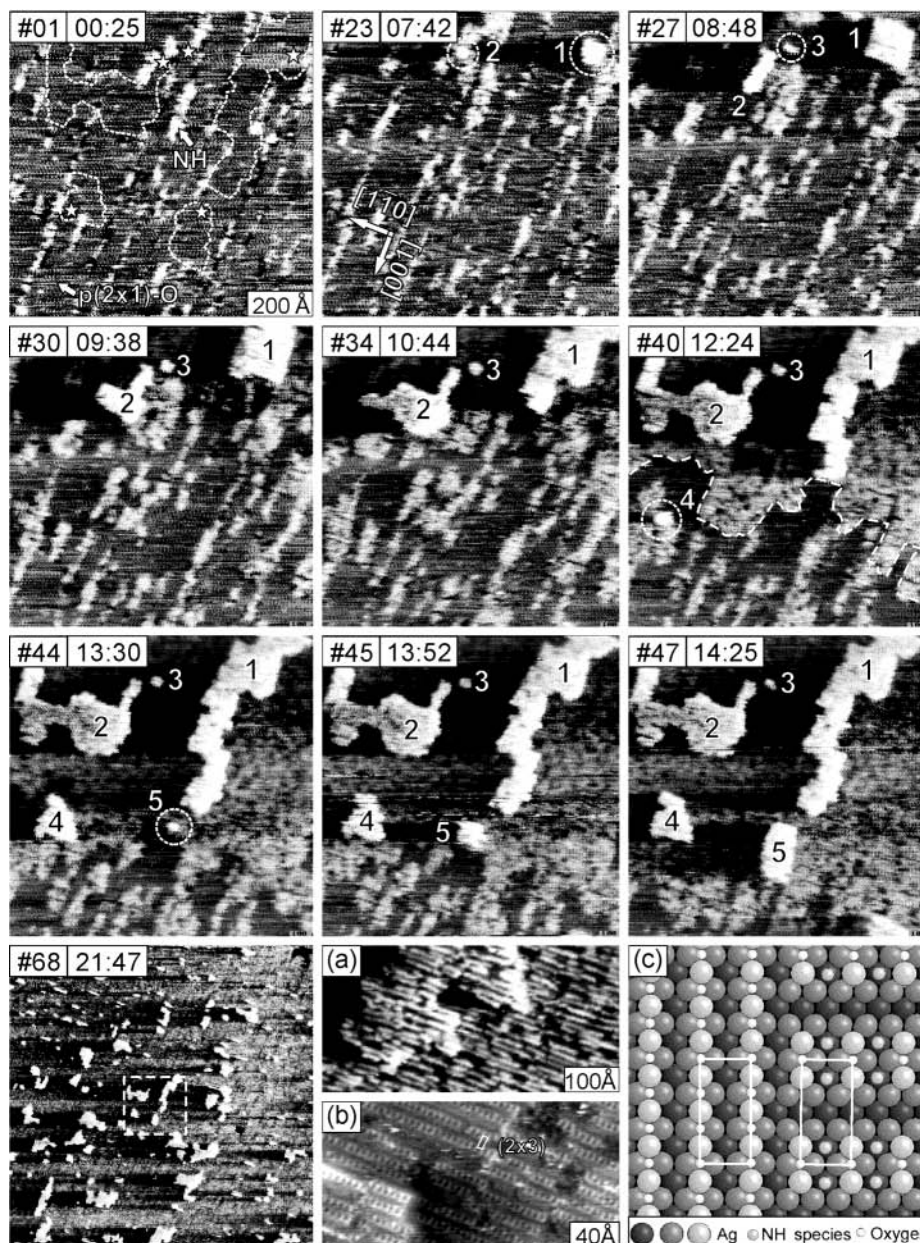


**FIGURE 6.** Selected frames of an STM movie recorded at 300 K during  $\text{NH}_3$  exposure of the  $\text{Ag}(110)\text{-p}(2\times 1)\text{-O}$  surface at 300 K. The scan rate was 16 s per frame. (a) Zoomed-in STM image showing  $\text{NH}(a)$  strands. (b) High-resolution STM image showing a  $(2\times 3)$  periodicity. (c) Structure model for  $\text{Ag}(110)\text{-p}(2\times 1)\text{-O}$  (left) and  $(2\times 3)\text{-NH}$  (right). $\times$

Many species incorporate metal atoms into their surface structures. Adsorbed atomic oxygen is but one example in which metal atoms are drawn from the surface to stabilize an atomically adsorbed species.  $\text{NH}(a)$  represents an example of the incorporation of metal atoms by a molecular fragment. To date we have found several other molecular intermediates that incorporate metal atoms; these include  $\text{NO}_3(a)$ ,<sup>35</sup> and  $\text{SO}_3(a)$ <sup>36</sup> on  $\text{Ag}(110)$ , and  $\text{SO}_3^-(a)$  on  $\text{Cu}(110)$ .<sup>11</sup> These processes have been reviewed recently elsewhere.<sup>37</sup>

## 7. Summary

During adsorption and reactions, the catalytic metal surfaces may undergo massive structural changes on the

nanometer scale due to the incorporation of metal atoms in the structures of intermediate species. Defects may be intimately involved in these processes. Adsorbates and reaction intermediates can move on the surface in a collective manner due to lateral interactions, requiring more advanced treatments of diffusion processes on surfaces. Amidst the restructuring and movement, reactive sites may be created and destroyed in a dynamic interplay. Without the direct, real-time observations made possible by STM the complexity of these surface processes would be difficult to imagine and impossible to confirm.

*The support of the National Science Foundation, Division of Chemistry, Electrochemistry and Surface Science Program is gratefully acknowledged.*

## References

- (1) Laidler, K. J. *The World of Physical Chemistry*; Oxford University Press: New York, 1993; pp 232–289.
- (2) Binning, G.; Rohrer, H.; Gerber, Ch.; Weibel, E. Surface Studies by Scanning Tunneling Microscopy. *Phys. Rev. Lett.* **1982**, *49*, 57–61.
- (3) Wintterlin, J.; Trost, J.; Renisch, S.; Schuster, R.; Zambelli, T.; Ertl, G. Real-Time STM Observations of Atomic Equilibrium Fluctuations in an Adsorbate System: O/Ru(0001). *Surf. Sci.* **1997**, *394*, 159–169.
- (4) The STM movies can be viewed at *Madix Group Website*, <http://www.stanford.edu/group/madix/>.
- (5) Hartmann, N.; Madix, R. J. Growth and Ordering of Cu–O Islands during Oxygen Adsorption on Cu(110) at 470. *Surf. Sci.* **2001**, *488*, 107–122.
- (6) Ertl, G. Untersuchung von Oberflächenreaktionen Mittels Beugung Langsamer Elektronen (LEED): I. Wechselwirkung von O<sub>2</sub> und N<sub>2</sub>O mit (110)-, (111)- und (100)-Kupfer-Oberflächen. *Surf. Sci.* **1967**, *6*, 208–232.
- (7) Chua, F. M.; Kuk, Y.; Silverman, P. J. Oxygen chemisorption on Cu(110): An Atomic View by Scanning Tunneling Microscopy. *Phys. Rev. Lett.* **1989**, *63*, 386–389.
- (8) Coulman, D.; Wintterlin, J.; Behm, R. J.; Ertl, G. Novel Mechanism for the Formation of Chemisorption Phases: The (2×1)O-Cu(110) “Added Row” Reconstruction. *Phys. Rev. Lett.* **1990**, *64*, 1761–1764.
- (9) Jensen, F.; Besenbacher, F.; Laegsgaard, E.; Stensgaard, I. Surface Reconstruction of Cu(110) Induced by Oxygen Chemisorption. *Phys. Rev. B* **1990**, *41*, 10233–10236.
- (10) Mocuta, D.; Ahner, J.; Lee, J. G.; Denev, S.; Yates, J. T. Self-organized nanostructures: an ESDIAD study of the striped organized Cu(110) surface. *Surf. Sci.* **1999**, *436*, 72–82.
- (11) Alemozafar, A. R.; Guo, X.-C.; Madix, R. J. Adsorption and Reaction of Sulfur Dioxide with Cu(110) and Cu(110)-p(2×1)-O. *J. Chem. Phys.* **2002**, *116*, 4698–4706.
- (12) Crew, W. W.; Madix, R. J. A Scanning Tunneling Microscopy Study of the Oxidation of CO on Cu(110) at 400 K: Site Specificity and Reaction Kinetics. *Surf. Sci.* **1996**, *349*, 275–293.
- (13) Habraken, F. H. P. M.; Bootsma, G. A. Kinetics of then Interactions of O<sub>2</sub> and N<sub>2</sub>O with Cu(110) Surface and of the reaction of CO with Adsorbed Oxygen Studied by Means of Ellipsometry, AES, and LEED. *Surf. Sci.* **1979**, *87*, 333–347.
- (14) Habraken, F. H. P. M.; Bootsma, G. A.; Hofmann, P.; Hachicha, S.; Bradshaw, A. M. Adsorption and Incorporation of Oxygen on Cu(110) and its Reaction with Carbon Monoxide. *Surf. Sci.* **1979**, *88*, 285–298.
- (15) van Pruijsen, O. P.; Dings, M. M. M.; Gijzeman, O. L. J. Surface and Subsurface Oxygen on Cu(111), Cu(111)-Fe, and Cu(110) and Their Influence on the Reduction with CO and H<sub>2</sub>. *Surf. Sci.* **1987**, *179*, 377–386.
- (16) Domagala, M. E.; Campbell, C. T. The Mechanism of CO Oxidation over Cu(110): Effect of CO Gas Energy. *Catal. Lett.* **1991**, *9*, 65–70.
- (17) Guo, X.-C.; Madix, R. J. In Situ STM Imaging of Ammonia Oxydehydrogenation on Cu(110): The Reactivity of Preadsorbed and Transient Oxygen Species. *Surf. Sci.* **1997**, *387*, 1–10.
- (18) Lackey, D.; Surman, M.; King, D. A. Adsorption of Ammonia on Cu(110). *Vacuum* **1983**, *33*, 867–869.
- (19) Afsin, B.; Davies, P. R.; Pashuski, A.; Roberts, M. W. The Role of a Dioxide Precursor in the Selective Formation of Imide NH(a) Species at a Cu(110) Surface. *Surf. Sci.* **1991**, *259*, L724–728.
- (20) Afsin, B.; Davies, P. R.; Pashuski, A.; Roberts, M. W. Reaction Pathways in the Oxydehydrogenation of Ammonia at Cu(110) Surfaces. *Surf. Sci.* **1993**, *284*, 109–120.
- (21) Carley, A. F.; Davies, P. R.; Roberts, M. W. The development of a new concept: the role of oxygen transients, defect and precursor states in surface reactions. *Catal. Lett.* **2002**, *80*, 25–34.
- (22) Guo, X.-C.; Madix, R. J. Nonuniform Product Inhibition in Surface Reactions: Spatial Organization Effects in Ammonia Oxydehydrogenation on Cu(110). *J. Chem. Soc., Faraday Trans.* **1997**, *93*, 4197–4200.
- (23) Guo, X.-C.; Madix, R. J. Site-Specific Reactivity of Oxygen at Cu(110) Step Defects: An STM Study of Ammonia Dehydrogenation. *Surf. Sci.* **1996**, *367*, L95–L101.
- (24) Leibsle, F. M.; Murray, P. W.; Francis, S. M.; Thornton, G.; Bowker, M. One-dimensional reactivity in catalysis studied with the scanning tunneling microscope. *Nature* **1993**, *363*, 706.
- (25) Leibsle, F. M.; Francis, S. M.; Davis, R.; Xiang, N.; S. H.; Bowker, M. Scanning tunneling microscopy studies of formaldehyde synthesis on Cu(110). *Phys. Rev. Lett.* **1994**, *72*, 2569.
- (26) Ruan, L.; Stensgaard, I.; Laegsgaard, E.; Besenbacher, F. The decomposition of ammonia on an oxygen-precovered Ni(110) surface studied by scanning tunneling microscopy. *Surf. Sci.* **1994**, *314*, L873–L878.
- (27) Coulman, D.; Wintterlin, J.; Behm, R. J.; Ertl, G. Novel mechanism for the formation of chemisorption phases: the (2×1) O-Cu 110 added-row reconstruction. *Phys. Rev. Lett.* **1990**, *64*, 1761–1764.
- (28) Wintterlin, J.; Schuster, R.; Coulman, D.; Ertl, G.; Behm, R. J. Atomic Motion and Mass Transport in the Oxygen Induced Reconstructions of Cu(110). *J. Vac. Sci. Technol., B* **1991**, *9*, 902–907.
- (29) Besenbacher, F.; Stensgaard, I. Review: Microscopic studies of adsorbate restructuring at metal surfaces. In *The Chemical Physics of Solid Surfaces*; King, D. A., Woodruff, D. P., Eds.; Elsevier: Amsterdam, 1993; Vol. 6, Chapter 15.
- (30) Nakagawa, N.; Komatsu, T. S. Collective Motion Occurs Inevitably in a Class of Populations of Globally Coupled Chaotic Elements. *Phys. Rev. E* **1998**, *57*, 1570–1575.
- (31) Tanaka, K. Atomic Scale Chemistry of Metal-Surface. *Jpn. J. Appl. Phys.* **1993**, *32*, 1389–1393.
- (32) Pai, W. W.; Reutt-Robey, J. E. Formation of (n×1)-O/Ag(110) Overlayers and the Role of Step-Edge Atoms. *Phys. Rev. B* **1996**, *53*, 15997–16005.
- (33) Guo, X.-C.; Madix, R. J. Structural and Morphological Changes Accompanying the Reaction of Ammonia with Ag(110)-p(2×1)-O: An STM Study. *Surf. Sci.* **2002**, *501*, 37–48.
- (34) Thornburg, D. M.; Madix, R. J. Cleavage of N–H Bonds by Active Oxygen on Ag(110). 1. Ammonia. *Surf. Sci.* **1989**, *220*, 268–294.
- (35) Guo, X.-C.; Madix, R. J. Microscopic Studies of NO<sub>2</sub> on Ag(110)-p(2×1)-O and Reactivity of Surface Nitrate. *Surf. Sci.* **2002**, *496*, 39–50.
- (36) Alemozafar, A. R.; Guo, X.-C.; Madix, R. J.; Hartmann, N.; Wang, J. Reaction of Sulfur Dioxide with Ag(110)-p(2×1)-O: A LEED, TPRS, and STM Investigation. *Surf. Sci.* **2002**, *504*, 223–234.
- (37) Guo, X.-C.; Madix, R. J. *J. Phys. Chem. B* **2002**, in press.

AR960308O